

Are More Complicated Tumor Control Probability Models Better?

Jiafen Gong*, Mairon, M. dos Santos, Chris Finlay, Thomas Hillen

Centre for Mathematical Biology
Department of Mathematical & Statistical Sciences
University of Alberta
Edmonton, AB, T6G 2G1, CANADA

June 27, 2011

Abstract

Mathematical models for the tumor control probability (TCP) are used to estimate the expected success of radiation treatment protocols of cancer. There are several mathematical models in the literature, from the simplest (Poissonian TCP) to well advanced stochastic birth-death processes. We made the experience that simple and complex models often make the same predictions, and hence, here, we present a systematic study where we compare six of these TCP models: the Poisson TCP, the Zaider-Minerbo TCP, a Monte Carlo TCP, and their corresponding cell cycle (two-compartment) models. Several clinical non-uniform treatment protocols for prostate cancer are employed to evaluate these models. These include fractionated external beam radiotherapies, and high and low dose rate brachytherapies.

Indeed, we find that in realistic treatment scenarios, all one-compartment models and all two-compartment models give basically the same results. A difference occurs between one-compartment and two-compartment models due to reduced radiosensitivity of quiescent cells. We find that care must be taken for the right choice of parameters, such as the radio-sensitivities α and β and the hazard function h . Typically, different hazard functions are used for fractionated treatment (fractionated survival fraction) and for brachytherapies (Lea-Catchside protraction factor). We were able to combine these two approaches into one *effective* hazard function.

Based on our results, we can recommend the use of the Poissonian TCP for every day treatment planning. More complicated models should only be used when absolutely necessary.

*Corresponding author: jgong@math.ualberta.ca

1 Background

A standard treatment for the control of tumor growth is radiation. Many mathematical models have been developed to help to predict the outcome of a given radiation treatment schedule. One such mathematical tool is the tumor control probability (TCP). The TCP is a measure for the probability of tumor cell eradication and it can be used to compare the expected success of different treatment protocols. The very nature of tumor control, i.e. the eradication of clonogenic cells, requires a stochastic approach for the TCP. There are several TCP models in the literature, which are based on Poisson statistics, on general birth-death processes, on branching processes, and on individual based models. Several of these models have been validated using clinical data ([33], [15]) hence we are confident about the significance of these models. While the first models in this class are based on a single clonogenic population ([46], [13]), extensions have been presented which aim to include cell cycle or quiescent states ([14], [23]). Some of these models are fairly simple (for example the Poissonian TCP), while other are very complex (for example a TCP model from a cell-cycle birth-death process). In practice it is hard to judge which of these models to use. What do we lose if we still use the simple model and not the more complicated alternatives?

The purpose of this paper is to show that, in realistic treatment scenarios for prostate cancer, all models give very similar results. Discrepancies can be observed, however, these are small compared to other uncertainties that are intrinsic in these models. Our conclusion is that the Poissonian TCP model is just good enough for every day treatment planning. In particular when it comes to the comparison of different treatment protocols. More complicated models should only be used if there is a striking reason to do so. This confirms theoretical results by Hanin [11], who showed that in the limit for large tumors and not too fast growing tumors the distribution of surviving tumor cells approximates a Poisson (or generalized Poissonian) distribution.

Some work has been done on the comparison of different TCP models: Tucker *et al.* [39] first questioned the efficacy of the Poissonian TCP by numerical simulation and found that the Poissonian TCP might underestimate the correct TCP. In an example of a very fast growing tumor the discrepancy was about 15%. Yakovlev [44] confirmed these findings theoretically, and Hanin and his group [13, 12, 11] proved, mathematically, that the TCP based on the iterative birth-death process converges to a Poissonian TCP for uniform fractionated treatment.

The six TCP models, which we compare in this paper are

(1-P): **The Poissonian TCP.** The Poissonian TCP is the standard formula for TCP computations for uniform fractionated treatments. There are several extensions of this model which include re-growth or lesion repair mechanisms and we discuss those later in Section 2.

(1-ZM): **The TCP of Zaider and Minerbo [46]:** The TCP of Zaider and Minerbo is based on a birth

death process for tumor growth and decay. It is the first model which allows for any temporal form of radiation treatment and the approach of Zaider and Minerbo has revolutionized the field.

(1-MC): **Monte-Carlo TCP.** Here we explicitly simulate a large number of cells and use Monte-Carlo simulations to estimate tumor survival.

(2-P): **two-compartment Poissonian TCP.** Here we aim to include cell-cycle mechanisms. For that we split the cell populations into two compartments which represent an active phase (G1, S, G2, M) and a quiescent phase (G0). If the clonogenic cells do not enter a G0 phase, then the model equally applies for a splitting into active (S, G2, M) and quiescent (G1) phases. The major assumption is that active cells are more radiosensitive compared to cells in the quiescent compartment.

(2-DH): **two-compartment TCP of Dawson and Hillen [6].** The Dawson and Hillen TCP is based on a birth-death process and generalizes of the ZaiderEt00 TCP to aim to include cell cycle effects according to the splitting mentioned in item 4.

(2-MC): **two-compartment Monte-Carlo TCP.** Here we extend the Monte-Carlo simulations to the two-compartment scenario.

These models depend on a number of parameters, for example the initial number of tumor cells n_0 , the radiation sensitivities α and β , or the so called "hazard function" $h(t)$. We will test several combinations of the parameter values and we give details about the models and parameters in Section 2. In Section 3 we present our results and we conclude the paper with a discussion in Section 4.

1.1 Prostate cancer

Prostate cancer is the most common malignant tumor afflicting men in the world [27]. Fortunately, early detection tests - such as digital rectal exam, or determining the amount of prostate-specific antigen (PSA) in the blood - increase the chance of early diagnosis and hence successful treatment [1]. One very important treatment method for prostate cancer is radiotherapy, where ionizing particles (such as X-rays and gamma-rays) transfer energy and kill cancer cells in the treated area. Over half of all cancer patients receive radiotherapy at some stage of their disease, either alone or in combination with other types of treatment (such as surgery or chemotherapy) [16, 25]. Two types of radiotherapy methods are available: brachytherapy, whereby a radiation probe is inserted into the tumor; and external beam radiotherapy, in which the tumor is irradiated from outside the patient. Generally speaking, in external beam radiotherapy, the total dose¹ is split into several fractions to allow the patient's normal tissues to recover between fractions.

¹energy per unit mass in unit of gray (Gy).

Brachytherapy is more efficient for early stage, localized prostate cancer. There are two brachytherapy methods for prostate cancer: high dose rate and permanent seeds (also called low dose rate) brachytherapy [4]. High dose rate brachytherapy involves inserting several fractions of seeds, over a span of a few days, through very tiny plastic catheters placed into the prostate gland. In low dose rate brachytherapy, seeds are injected into the glands. These seeds will irradiate off at a low dose rate and remain in the gland for a long time. If we denote the initial dose as R_0 and the seed decay rate as λ , then the total dose $D(t)$ absorbed up to time t is given by

$$D(t) = \frac{R_0}{\lambda}(1 - e^{-\lambda t}). \quad (1.1)$$

2 TCP Models

Before we introduce the TCP models, we briefly discuss the linear quadratic model for cell survival and the hazard function.

2.1 Survival Fraction

If D denotes the radiation dose, then we denote the survival fraction of cells as $S(D)$. A widely accepted survival fraction model is the linear-quadratic model (LQ):

$$S(D) = \exp(-\alpha D - \beta D^2), \quad (2.2)$$

where α (Gy^{-1}) and β (Gy^{-2}) are radiosensitivity parameters depending on the tissue types. The parameters α and β are empirically estimated parameter values and they include radio sensitivity as well as repair mechanism. The ratio α/β is a rough characterization of the sensitivity of tissues to radiation and it can be used to differentiate tissues into early responding tissue ($\alpha/\beta \approx 10$, typical for clonogenic tissue) or late responding tissue (the ratio is about 3, typical for healthy tissue) [41] [7]. When the treatment dose D is split into n fractions of dose d , $D = nd$ and the survival for each fractions is independent, (2.2) changes into

$$S(D(n, d)) = \underbrace{\exp(-\alpha d - \beta d^2) \cdots \exp(-\alpha d - \beta d^2)}_n = \exp(-\alpha D - \beta d D) = \exp(-(\alpha + \beta d)D). \quad (2.3)$$

Equations (2.2) and (2.3) assume there is no regrowth during treatment. However proliferation plays an important role when the treatment time is long compared to the tumor doubling time. Travis and Tucker [38] were the first to include a time factor in the LQ model. By fitting mouse lung cancer data of Mah *et al.* [22], they found the regrowth is exponential with parameter b , and the isoeffect curves E ($= -\ln S(D)$) are constant,

$$E = \beta D(\alpha/\beta + D/n) - bT, \quad (2.4)$$

where n is the number of fractions and T is the total treatment time. Some other scholars [21, 36, 42, 43] also study regrowth and regrowth delay in the LQ models. Therefore by using this exponent in the LQ model, we have an LQ model as a function of dose and time,

$$S(D, t) = e^{-\alpha D - \beta D^2/n} e^{\frac{\ln(2)}{T_d}(t-t_k)}. \quad (2.5)$$

where $T_d = \ln(2)/b$ is the tumor doubling time and t_k is a time delay between the beginning of treatment and measurable re-growth of the tumor.

In Brachytherapy (continuous radiation over time), the model is modified using the Lea-Catcheside factor $G(t)$ [17]

$$S(D) = e^{-\alpha D - \beta G(t)D^2}. \quad (2.6)$$

The Lea Catchside factor describes the interaction of past radiation damage with current damage, where the interaction probability decays exponentially with rate γ . The Lea Catchside factor is usually written for $t > T$ as

$$G(t) = \frac{2}{D(t)^2} \int_{-\infty}^{\infty} \dot{D}(\tau) \int_{-\infty}^{\tau} e^{-\gamma(\tau-s)} \dot{D}(s) ds d\tau$$

or

$$G(T) = \frac{2}{D(T)^2} \int_{-\infty}^T \dot{D}(\tau) \int_{-\infty}^{\tau} e^{-\gamma(\tau-s)} \dot{D}(s) ds d\tau,$$

where $\dot{D}(t)$ is the dose rate, $D(t)$ is the cumulative dose, and T denotes the end of treatment. The Lea-Catcheside factor for endpoints $t > T$ has a clear physical derivation from a model of lesion damage and lesion repair (see [?]). Another approach, which is also based on clear physical principles, is the assumption of an effective interaction window for lesions ([6]). If two single hit events occur close in time, then there is a chance of an interaction. In this case the survival fraction reads

$$S(D) = \exp\left(-\int_0^t [\alpha + \beta(D(s) - D(s - \omega))\dot{D}(s)] ds\right),$$

where ω denotes the size of the effective interaction window.

2.2 Hazard Function

We can use the concept of a hazard function to unify the above models into one formalism. The hazard function $h(t)$ describes the decay of survival fraction as

$$\frac{dS(D(t))}{dt} = -h(t)S(D(t)). \quad (2.7)$$

Zaider and Minerbo advertise the following hazard function for any form of treatment

$$h_1(t) := (\alpha + 2\beta D(t))\dot{D}(t) \quad (2.8)$$

If we solve for the surviving fraction according to the model (2.7) we obtain

$$S(D(t)) = \exp\left(-\int_0^t h(s)ds\right) = \exp(-\alpha D(t) - \beta D^2(t)). \quad (2.9)$$

Case 1: If we only give one treatment of dose d and evaluate the above formula at the end of treatment T , then we get

$$S(D(T)) = e^{-\alpha d - \beta d^2},$$

which is the LQ model.

Case 2: If, however, we give n fractions of dose d , then at the end of treatment we obtain

$$S(D(T)) = \exp(-\alpha nd - \beta (nd)^2) \quad (2.10)$$

which does not correspond to the fractionated LQ formula (2.3). In (2.10) the β -term is over-amplified by an additional factor of n , which, as we argue, leads to over optimistic estimates for the TCP.

Based on (2.8) we rather propose the following form of hazard function for fractionated treatment:

$$h_2(t) := (\alpha + \beta d)\dot{D}(t). \quad (2.11)$$

The term $\beta d\dot{D}(t)$ describes the interaction of previous lesions with current radiation, which is on a small time scale compared to the treatment time T . If we solve (2.7) using $h_2(t)$, we obtain

$$S(D(t)) = \exp(-(\alpha + \beta d)D(t)),$$

which is exactly the LQ model (2.3).

In more generality, we propose an effective interaction dose d_{eff} , which then will include the Lea-Catchside factor, the fractionated schemes from above and the interaction window approach into one framework:

$$h_3(t) := (\alpha + \beta d_{\text{eff}}(t))\dot{D}(t), \quad (2.12)$$

where

- (a) $d_{\text{eff}} = d$ for fractionated treatments,
- (b) $d_{\text{eff}}(t) = 2D(t)$ as in Zaider-Minerbo's formula (2.9),
- (c) $d_{\text{eff}}(t) = 2 \int_{-\infty}^t e^{-\gamma(t-s)} \dot{D}(s) ds$ for the Lea-Catchside factor, and
- (d) $d_{\text{eff}}(t) = 2(D(t) - D(t - \omega))$ for the finite interaction window.

The corresponding survival fractions are then

$$S(D(t)) = \exp\left(-\alpha D(t) - \beta \int_0^t d_{\text{eff}}(s)\dot{D}(s)ds\right)$$

Then we compute

$$(a) \quad S_a(D(t)) = \exp(-(\alpha + \beta d)D(t)) \quad (2.13)$$

$$(b) \quad S_b(D(t)) = \exp(-\alpha D(t) - \beta D^2(t)) \quad (2.14)$$

$$(c) \quad S_c(D(t)) = \exp(-\alpha D(t) - \beta G(t)D(t)^2), \text{ with } G(t) \text{ from (2.17)} \quad (2.15)$$

$$(d) \quad S_d(D(t)) = \exp\left(-\alpha D(t) - \beta \int_0^t 2(D(s) - D(s - \omega))\dot{D}(s)ds\right), \quad (2.16)$$

There are several interesting special cases:

Case 1: If we consider fractionated treatment, and the interval ω includes one fractionation then we can compute the integral in case (d) and find $S_d(t) = S_a(t)$ which is in agreement with the LQ-model.

Case 2: If $\gamma \rightarrow 0$ in (c), then $d_{\text{eff}}(t) = 2D(t)$ and we obtain the Zaider-Minerbo formula (b). This shows that the approach (b) is useful if early lesions are not repaired and are always able to interact.

Case 3: If the interaction window in (d) is large ($\omega \rightarrow \infty$) we use the fact that $D(-\infty) = 0$ to see that (d) corresponds to (b). Hence we get the same picture as in Case 2 above; model (b) implicitly assumes that interactions of radiation induced lesions are on a long time scale.

Case 4: If the interaction window is small ($\omega \rightarrow 0$) then we redefine: $\tilde{\beta} = \beta\omega$ and we obtain

$$h_3 \rightarrow (\alpha + \tilde{\beta}\dot{D}(t))\dot{D}(t).$$

In this scenario, interactions would be strictly local in time.

Case 5: The Lea-Catchside factor has originally been derived from a lethal-potentially lethal model (LPL model) (see [17]) for an end point that is well after treatment $t > T$. We can, however, use the same LPL model to derive a time-dependent Lea-Catchside factor, which applies to all times $t > 0$. This formulation leads to our choice of $d_{\text{eff}}(t)$ in (c). In that case, the Lea-Catchside factor becomes:

$$G(t) = \frac{2}{D(t)^2} \int_{-\infty}^t \dot{D}(\tau) \int_{-\infty}^{\tau} e^{-\gamma(\tau-s)} \dot{D}(s) ds d\tau, \quad (2.17)$$

In the sequel, we will compare these different forms of hazard functions for the six models mentioned above. We find that the results for (c) Lea-Catchside and (d) finite interaction window are virtually identical, while case (b) gives over-optimistic results.

2.3 Poissonian TCP

The simplest TCP models are based on the Poisson or the Binomial distribution and the linear quadratic survival fraction model. They both assume that the initial number of tumor cells N_0 is large. Let X denote a random variable for the amount of surviving cells. If the death of tumor cells is stochastically independent of each other, and cell survival is a rare event, then we can assume X is given by the Poisson distribution. The probability of k tumor cells surviving is then,

$$p(X = k) = \frac{\lambda^k e^{-\lambda}}{k!}. \quad (2.18)$$

Since the expectation of this distribution is $E(X) = \lambda$, we use the number of surviving cells $N_0 S(D)$ as an estimator for λ . Therefore we have the Poisson TCP as

$$TCP_P = p(X = 0) = e^{-\lambda} = e^{-N_0 S(D)}. \quad (2.19)$$

Similarly, the Binomial TCP has the form,

$$TCP_B = (1 - S(D))^{N_0}, \quad (2.20)$$

if the number of surviving cells X satisfies a Binomial distribution. The Poisson approximation tells us that the Binomial distribution approaches the Poisson distribution when $N_0 \rightarrow \infty$, $S(D) \rightarrow 0$ and the product of $N_0 S(D)$ approaches the constant λ (i.e. $N_0 S(D) \rightarrow \lambda$).

To include cell regrowth, we generalize equation (2.5), which is based on linear regrowth

$$\frac{dN}{dt} = (b - d)N(t), \quad (2.21)$$

where b denotes the mitosis rate and d the natural death rate. A more general form of cell growth is given by a Bernoulli model [40]

$$\frac{dN}{dt} = \frac{bN}{a} \left[1 - \left(\frac{N}{\theta} \right)^a \right]. \quad (2.22)$$

Here the parameters a (≥ 0), b and θ (> 0) are determined from the growth characteristics of the cells. We can easily see that the exponential growth model arises when $a \rightarrow 1$ and $\theta \rightarrow \infty$. The logistic growth model follows when $a \rightarrow 1$ and the Gompertzian growth model follows when $a \rightarrow 0$. Combined with a hazard function for radiation treatment we obtain the following ODE model for the tumor cell population

$$\frac{dN}{dt} = \frac{bN}{a} \left[1 - \left(\frac{N}{\theta} \right)^a \right] - h(t)N. \quad (2.23)$$

Again, we estimate the parameter λ in the Poisson distribution (2.19) as the expected number of surviving tumor cells and obtain the one-compartment Poissonian TCP

$$TCP_{P_1}(t) = e^{-N(t)}. \quad (2.24)$$

In [9], we derive an explicit formula for non-uniform treatments: treatments with breaks over the weekend. It is considerably more complex than (2.3), since we need to keep track of different time intervals (weekday versus weekend). Nevertheless, a formula can be obtained and we refer to [9] for details.

The two-compartment Poisson TCP can be calculated by the following system of ODEs for active (a) and quiescent cells (q) ([14]),

$$\frac{da}{dt} = -\mu a + \nu q - (d_a + h_a(t))a \quad (2.25)$$

$$\frac{dq}{dt} = 2\mu a - \nu q - (d_q + h_q(t))q. \quad (2.26)$$

Here h_a and h_q are the hazard functions for active and quiescent cells and d_a, d_q are the natural death rates, respectively. The term μ gives the regrowth rate of active cells, and ν gives the switch rate of quiescent cells to active cells. We solve it numerically, and then evaluating

$$TCP_{P_2}(t) = e^{-(a(t)+q(t))}. \quad (2.27)$$

The two compartment model in (2.25, 2.26) is based on a more general two compartment model in [14]. The model in [14] allows cells after mitosis to become quiescent, or to continue in the cell cycle. Two special cases lead to the one-compartment model (2.21) on the one hand, and two the two-compartment model (2.25,2.26) on the other hand. In this paper we focus on these two extreme cases. For a full discussion of the two compartment models we refer to the literature [6, 14].

2.4 TCP Based on Birth-Death Processes

When the number of tumour cells are small, stochastic effects dominate. In this case, deterministic models seem to be inappropriate for predicting the number of surviving cells. To accommodate the stochastic effects, Zaider and Minerbo [46] employed a stochastic birth-death process. That is, the probability P_i of i tumour cells surviving at time t is given by the master equation

$$\frac{dP_i(t)}{dt} = (i-1)bP_{i-1}(t) - i(b+d+h(t))P_i(t) + (i+1)(d+h(t))P_{i+1}(t), \quad i = 0, 1, 2, 3, \dots \quad (2.28)$$

with the convention that $P_{-1} = 0$. The expected number of tumor cells $N(t) = \sum i P_i(t)$ satisfies the mean field equation

$$\frac{dN(t)}{dt} = [b - d - h(t)] N(t), \quad N(0) = N_0. \quad (2.29)$$

The mean-field description (2.29) of tumour cell proliferation and its death due to radiation is a reasonable approach when the number of cells is large. However, for a relatively small cell-population (e.g., at the end of the treatment), the average behavior is no longer adequate as probabilistic or stochastic noise becomes dominant.

By introducing a generating function, Zaider & Minerbo solve the master equation (2.28) and obtain an explicit expression for the tumour control probability,

$$TCP_{ZM}(t) = P_0(t) = \left[1 - \frac{S_h(t)e^{bt}}{1 + bS_h(t)e^{bt} \int_0^t \frac{dr}{S_h(r)e^{br}}} \right]^{N_0}. \quad (2.30)$$

Here

$$S_h(t) = \exp\left(-\int_0^t d + h(r) dr\right) \quad (2.31)$$

is the probability of cell survival for a given hazard function $h(t)$ and natural death rate d . In [6], Dawson and Hillen simplified the Zaider-Minerbo TCP into

$$TCP_{ZM}(t) = \left[1 - \frac{N(t)}{N_0 + bN_0N(t) \int_0^t \frac{dr}{N(r)}}\right]^{N_0}, \quad (2.32)$$

where N solves the mean field equation (2.29). Note that when $b = 0$, the Zaider-Minerbo TCP reduces to the binomial TCP.

In the previous section we discussed the use of a two-compartment model to describe cell-cycle effects. This extension can also be done for the birth-death process of Zaider and Minerbo (see Dawson and Hillen [6], Hillen *et al.* [14], McAneney *et al.* [28]). The basic idea is the same as above, i.e. a detailed Master equation for two compartments is used as a starting point. The mean-field equations are given by equations (2.25, 2.26) and the tumor control probability can again be expressed by the corresponding solutions of the mean field equations. The resulting TCP_{DH} formula is very complex and we refer to the original papers for reference ([6], [14]).

2.5 Monte Carlo Method

Another class of models for tumor growth are individual based models (e.g. [?], [?]). Here we use the Monte Carlo method as representative for this class of models. The Monte Carlo method allows us to explicitly model the stochastic nature of cell - radiation interaction, cell proliferation and cell death. For the Monte Carlo simulations we use the same birth and death probabilities as used in the Master equation approach (2.28). The probability distributions for the random sampling in each time interval Δt is given by:

- $b\Delta t$ for the probability of regrowth in a time interval of length Δt , where b is the cell growth rate;
- $(d + h(t))\Delta t$ for probability of death in a time interval of length Δt , where $h(t)$ is the hazard function (2.12);
- $1 - (d + b + h(t))\Delta t$ is the probability the cell remains unchanged in a time interval of length Δt .

For each simulation run and for each time-step we define the treatment success indicator (TS) r as:

$$TS(t) = \begin{cases} 0, & \text{if } N(t) > 0 \\ 1, & N(t) = 0. \end{cases}$$

where $N(t)$ is the number of tumor cells at time t . The tumor control probability (TCP) is therefore defined as the average of M independent such simulations and given by

$$TCP(t) = \frac{1}{M} \sum_{i=1}^M TS_i(t). \quad (2.33)$$

According to the law of large numbers, the error after M samplings is the order of $1/\sqrt{M}$. In order to keep this error on an acceptable level, we we simulate each case 300 times and the outcome is averaged. The output of the TCP curve as a function of time is relatively smooth, with a small standard deviation (≈ 0.05).

For the two-compartment models, we have two subpopulations governed by their own probability distributions according to Table 3.2:

- $\mu\Delta t$ for the probability of regrowth in a time interval of length Δt , where μ is the cell growth rate;
- $(d_a + h_a(t))\Delta t$ and $(d_q + h_q(t))\Delta t$ for probability of death in a time interval of length Δt for the active and the quiescent cells, respectively, and $h_a(t)$, $h_q(t)$ are their hazard functions;
- $\nu\Delta t$ for the transition probability from quiescent into active cells in a time interval of length Δt ;
- $1 - (\mu + d_a + h_a(t))\Delta t$ and $1 - (\nu + d_q + h_q(t))\Delta t$ are the probabilities that the cells remain unchanged in a time interval of length Δt for the active and the quiescent cells, respectively.

The main drawback of the Monte Carlo method lies in its random nature: all the results are affected by statistical uncertainties which can be reduced at the expense of increasing the sample population and, hence, the computation time. This method is very convenient when the system has several degrees of freedom such as fluids [31] and cellular structures [8], or when inputs are very uncertain, such as risk in business [24]. More broadly Monte Carlo simulations have been applied to species dynamics in ecology, spatial sciences and oil exploration [10, 30].

3 Treatment Protocols and Parameter Values

In this section, we use seven treatment protocols for prostate cancer from the literature to compare the six models described in the previous section. Among them, three are standard treatments (labeled as A, C, D). These are given once per day on weekdays with weekends off. The others are one hyperfractionated treatment (labeled as e), one high dose rate brachytherapy (labeled as f) and two permanent seed brachytherapies (^{103}Pd , ^{125}I) (see Table 3.1).

For computational simplicity, we assume that all radiation protocols start on a Monday. Fractionated treatments A, C, D, e and f are given on weekdays with weekends off. We assume it takes 10 minutes

Protocol	Dose/frac.(d gray)	days/week	Total days	Times/day	Total dose	Reference
A	2	5	53	once	78	[32]
C	3	5	26	once	60	[2]
D	4.3	5	16	once	51.6	[20]
e	1.2	5	44	twice	76.8	[29]
f	6	5	4.5	twice	54	[45]

Protocol	Init. Dose	Decay Rate λ	Total days	Half Times	Total dose	Reference
^{103}Pd	5.71	0.0408	47.63	16.99	120	[26]
^{125}I	1.86	0.0117	207.8	59.4	145	[26]

Table 3.1: Seven treatment schedules for prostate cancer. A, C, D are standard treatments and e, f are two hyperfractionated treatments where f is a high dose brachytherapy, and $^{103}Pd, ^{125}I$ are two permanent seeds brachytherapy treatments. Note that the brachytherapy treatments have no end time, since the radioactive seeds remain in the body. The column "Total days" indicates the time when the total treatment dose is reached.

to deliver each fraction of the dose at a constant dose rate. If the protocols prescribe one fraction per day (called standard treatments), treatments are delivered at 12pm (noon); in the case of two fractions per day (called hyperfractionated treatments), treatments are delivered at 12 pm and 6 pm.

To compare parameter values between one- and two-compartment models, we use weighted averages. In the two-compartment model (2.25) and (2.26), the transition rate from active to quiescent is μ and the transition rate for quiescent to active is ν . Hence, assuming Poisson process for the transition events, the average time spent in the active phase is $1/\mu$ and in the quiescent phase $1/\nu$ (see [37]). The parameter values will be different for active and quiescent compartments, for example the β -value of the radiosensitivities. In general, let p_{one} be a parameter in the one-compartment model and p_a, p_q parameters for active and quiescent cells, respectively. Then the parameters are related by the following equation

$$p_{one} = p_a \frac{1/\mu}{1/\mu + 1/\nu} + p_q \frac{1/\nu}{1/\mu + 1/\nu}. \quad (3.34)$$

The parameters used in the two-compartment model are listed in the TCP_{DH} column in Table 3.2, and the parameters for the one-compartment model are in column TCP_{ZM} . In most publications on cancer growth the effective net growth rate is reported. We use this to estimate these values to estimate the net growth rate $b - d$. The parameters of the one-compartment models are related to the parameters of the two-compartment model via the weighted averaging described above (3.34). We will see later that this is indeed a good choice as the models behave quite similar.

The permanent seeds have dose rate $\dot{D}(t) = R_0 e^{-\lambda t}$, which is a continuous function of time t . In the case of fractionated treatments (protocols A, C, D, e and f from Table 3.1), $\dot{D}(t)$ are jump functions. Because of the differences in the dose rates, we report their results separately.

	TCP_{ZM}	TCP_{DH}	Unit	Reference
Init. cell	$N(0) = 10^{6*}$	$a(0) + q(0) = 10^6$	cells	[34]
net growth rate	$b - d = 0.0273$	$\mu - d_a = 0.0655$	1/day	[35]
		$\nu - d_q = 0.0476$	1/day	[3]
α	$\alpha = 0.1531$	$\alpha_a = 0.145$	Gy^{-1}	[5]
		$\alpha_q = 0.159$	Gy^{-1}	[5]
β	$2\beta = 2 * 0.0149$	$2\beta_a = 0.070646$	Gy^{-2}	[5]
		$2\beta_q = 0$		Assumption

Table 3.2: Table of parameters and references. Column TCP_{DH} refers to the two-compartment model, μ is the birth rate of its active tumor cells and ν is the transition rate from quiescent into active cells. $\alpha_a, \beta_a, \alpha_q, \beta_q$ are radiosensitive parameters of the LQ model for active and quiescent cells respectively. Column TCP_{ZM} refers to the one-compartment models, values are calculated from those in column TCP_{DH} by weighted averaging Equation (3.34). Besides the initial tumor size 10^6 , we also simulate for $N(0) = 10^2, 10^4, 10^5, 10^{10}$, which all give similar results, hence we choose to only present the result for 10^6 .

4 Results

4.1 Fractionated Treatments

In Figure 4.1 we show the time course of the tumor control probability for the three one-compartment models (1-P), (1-ZM), (1-MC). The five subplots refer to the five fractionated treatments A, C, D, e and f , where the vertical line indicates the end-time of these treatments. Within each figure we show two groups of three curves. The left group of three curves corresponds to the survival fraction described by (2.14), whereas the right group of curves corresponds to the survival fraction for fractionated treatments (2.13). Instead of using (2.13) directly, we use (2.16), which is equivalent with (2.13) for fractionated treatment, as mentioned earlier. This choice allows us later to use the same formulation for brachytherapy as well as for any other time-dependent treatment method. In [19], the best estimate of the average tumor DNA repair time is 16 minutes. That is to say, one DNA damage can only interact with another to create a double strand break, if they occur within 16 minutes. Hence we choose an interaction window of $\omega = 16 \text{ min}$, such that any dose delivered to a patient within this window will count towards the hazard function, as Dawson and Hillen [6] proposed.

The simulations clearly show that the three models make the same predictions. The hazard function (2.8) shows clearly over-optimistic results, while the results using the effective interaction dose d_{eff} are more plausible. The computation of absolute TCP values is not the point of this paper. The point is to show that these three very different methods show virtually identical TCP predictions. Hence they are equally useful for treatment outcome predictions.

In Figure 4.2 we plot the TCP's as function of dose. Again, we see that the curves that correspond

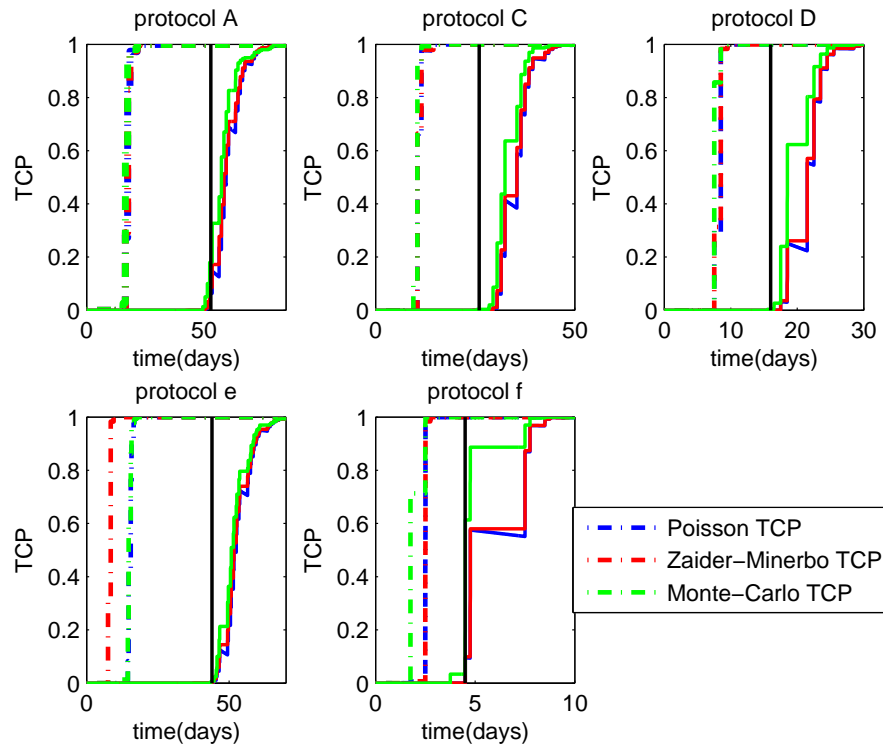


Figure 4.1: TCP for treatment A, C, D and e, f as function of time, with survival fraction (2.14) (and corresponding hazard function (2.8)) and survival fraction (2.13) (or equivalently (2.16)). Each subplot shows two groups of three curves. The left groups correspond to (2.14) while the right group corresponds to (2.13). The vertical line on each subplot is the treatment ending time. Blue lines are for Poissonian TCP (1-P), cyan lines for Zaider-Minerbo TCP (1-ZM) and red for Monte Carlo TCP (1-MC). All the parameter values are from Table 3.2.

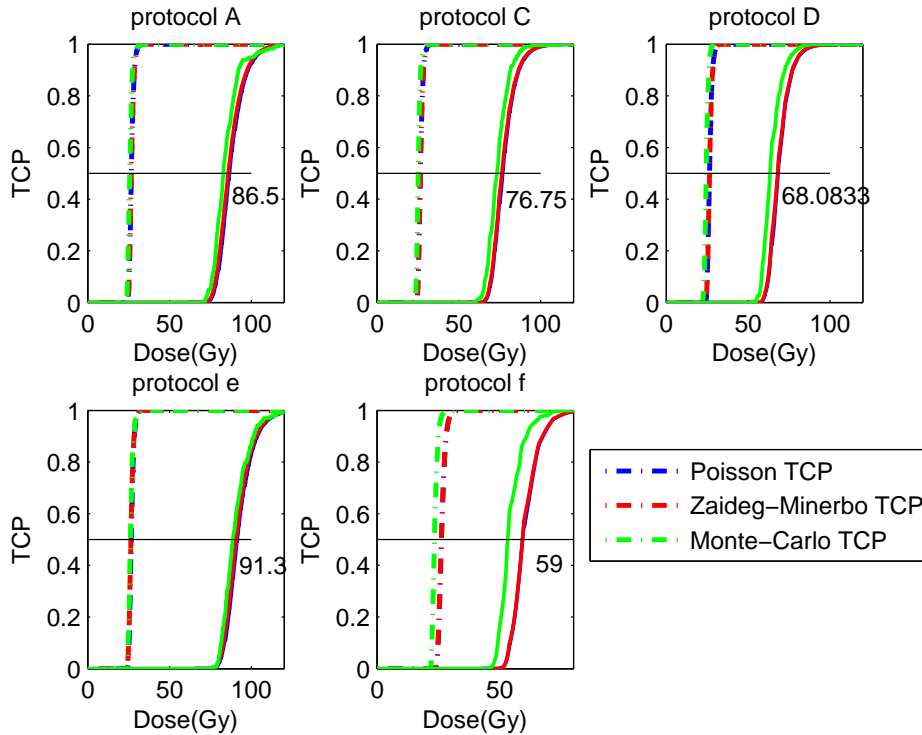


Figure 4.2: TCP for treatment A, C, D and e, f as function of dose, with survival fraction (2.14) (and corresponding hazard function (2.8)) and survival fraction (2.13) (or equivalently (2.16)). Each subplot is for one of the treatment protocol with results by using (2.14) gathering on the left part of each subplot and those with (2.13) sitting on the right part. Horizontal line denote the D_{50} position where $TCP = 0.5$. Blue lines are for Poissonian TCP, cyan lines for Zaider-Minerbo TCP and red for monte carlo TCP. All the parameter values are from Table 3.2.

to the same choice of $h(t)$ are very close. The numbers in each subplot are the D_{50} -value for the Poissonian TCP. We do not show the D_{50} -values for the other models, since they are very close as we can see from the graph. We compared our D_{50} values with those reported by Levegrun *et al* [18] from clinical data for prostate cancer. Our values for C, D, f are all in the 95% confidence intervals of their D_{50} values. Our D_{50} -values for A, e are a bit higher than the values reported by Levegrun *et al.* [18].

We also compare the three one-compartment models with their two-compartment models by using the parameters from Table 3.2. The results for protocols C and e are reported in Figure 4.3. We find that the difference between the one-compartment and two-compartment models are negligible for hyperfractionated treatment e ; while for standard treatment schedules C two-compartment TCPs are shifted to the right by at most 5 days. We have similar results for the other treatment protocols. Hence the existence of a quiescent compartment allows clonogenic cells to sequester from radiation and repopulate the tumor between treatments.

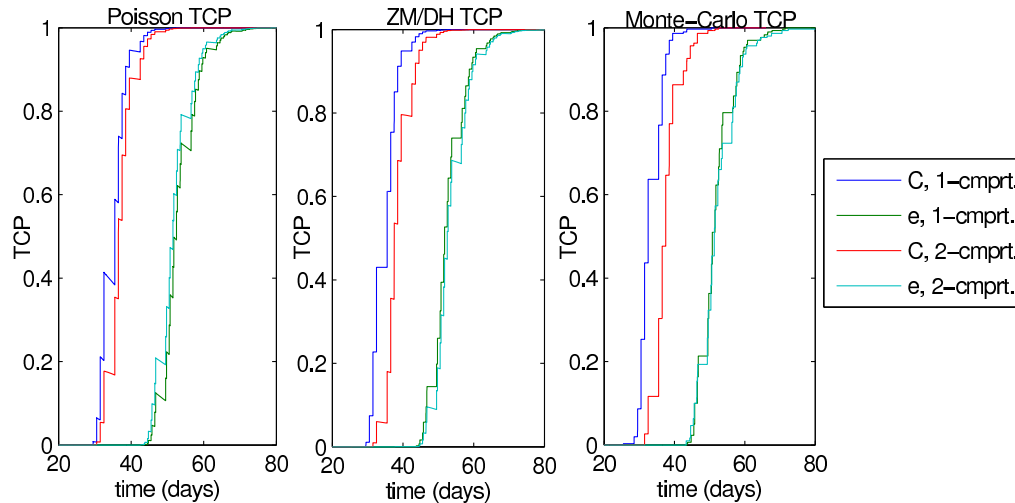


Figure 4.3: TCP as a function of time, using protocols C & e , for both the one- and two-compartment models. The left panel is for the Poisson TCPs ((1-P) and (2-P)), the middle panel is for the Zaider-Minerbo and Dawson-Hillen TCPs (1-ZM) and (2-DH)) and the right panel is for the Monte Carlo TCPs (1-MC) and (2-MC)). All parameters are taken from Table 3.2 and the *effective dose* hazard function (2.12)(d) is used.

4.2 Brachytherapy Treatments

A standard model for brachytherapy treatments is the hazard function with the Lea-Catcheside protraction factor (2.12) (c) and survival fraction (2.15). We will show that this choice of hazard function can be approximated by the effective interaction window hazard function (2.12) (d) and survival fraction (2.16). The Lea-Catcheside protraction factor is simple enough to program directly. However, by using the time-window approach, we will be able to find a hazard function which is equally applicable to fractionated therapies and to brachytherapy.

Choosing the total dose as for a radioactive seed as in (1.1), the Lea-Catcheside factor (2.17) can be explicitly computed as

$$G(t) = \frac{2R_0^2}{D(t)^2(\gamma - \lambda)} \left[\frac{1 - e^{-2\lambda t}}{2\lambda} + \frac{e^{-(\lambda+\gamma)t} - 1}{\lambda + \gamma} \right]. \quad (4.35)$$

Once again, R_0 is the initial dose rate, $D(t)$ is the total dose absorbed, λ is the average half-life for the permanent seed and $\omega = \ln(2)/\gamma$ is the life time of the DNA double strand breaks, which was chosen to be the same as in the *effective dose*, 16 minutes. In what follows, we show mathematically that the *effective dose* hazard function and Lea-Catcheside hazard function are almost the same, when both have the same parameters.

From (2.7) we can compute the Lea-Catcheside hazard function as

$$h_{LC}(t) = \frac{dS_{LC}(t)/dt}{-S_{LC}(t)} = \alpha D(t) + \beta \frac{d(G(t)D(t)^2)}{dt} = \alpha R_0 e^{-\lambda t} + \beta \frac{2R_0^2}{\gamma - \lambda} (e^{-2\lambda t} - e^{-(\lambda+\gamma)t}). \quad (4.36)$$

where we use Equation (4.35) in the last equality.

update the following computations with the inclusion of the right factor 2 in (2.12)(d)

By using the formula (1.1) in (2.12)(d), we have an *effective dose* hazard function as follows

$$h_{eff}(t) = \alpha R_0 e^{-\lambda t} + 2\beta \frac{R_0^2}{\lambda} (e^{-2\lambda t + \lambda \omega} - e^{-2\lambda t}). \quad (4.37)$$

The difference between $h_{eff}(t)$ and $h_{LC}(t)$ is

$$\begin{aligned} \frac{h_{eff}(t) - h_{LC}(t)}{2\beta R_0^2} &= \frac{e^{-2\lambda t + \lambda \omega} - e^{-2\lambda t}}{\lambda} - \frac{e^{-2\lambda t} - e^{-(\gamma + \lambda)t}}{\gamma - \lambda} \\ &= \frac{e^{-2\lambda t + \lambda \omega}(\gamma - \lambda) - e^{-2\lambda t}(\gamma - \lambda) - \lambda e^{-2\lambda t} + \lambda e^{-(\gamma + \lambda)t}}{\lambda(\gamma - \lambda)} \\ &= \frac{e^{-2\lambda t + \lambda \omega}(\gamma - \lambda) - \gamma e^{-2\lambda t}}{\lambda(\gamma - \lambda)} + \frac{e^{-(\gamma + \lambda)t}}{\gamma - \lambda} \\ &= e^{-2\lambda t} \left[\frac{e^{\lambda \omega}}{\lambda} - \frac{\gamma}{\lambda(\gamma - \lambda)} \right] + \frac{e^{-(\gamma + \lambda)t}}{\gamma - \lambda} \end{aligned}$$

Because $\gamma = \ln(2)/\omega = 62.38 \gg \lambda$, we have the following estimate

$$|h_{eff} - h_{LC}| \leq 2\beta R_0^2 \left| e^{-2\lambda t} \left(\frac{e^{\lambda \omega}}{\lambda} - \frac{1}{\lambda} \right) + \frac{e^{-(\gamma + \lambda)t}}{\gamma - \lambda} \right| \leq 2\beta R_0^2 \left| \frac{e^{\lambda \omega}}{\lambda} - \frac{1}{\lambda} + \frac{1}{\gamma - \lambda} \right| \quad (4.38)$$

The last expression equals 0.0626 for ^{103}Pd and 0.0066 for ^{125}I , when using the parameters in Table 3.2. Hence the difference between those two approaches is very small. We show numerical simulations of our three one-compartment models for these two types of hazard functions in Figure 4.4 and we find them to be indistinguishable. Also, if we compare the TCP for the three models (1-P), (1-ZM), (1-MC), they are also virtually identical, hence they give the same predictions.

Note that the ^{103}Pd curves for the Poissonian model do start to decay after about 110 days. The Poisson TCP formula is based on the mean field differential equations and consequently, the number of tumor cells can never be identical to zero. Hence after radiation subsides, the tumor will re-grow. The other two models (1-ZM), (1-MC) have the advantage that the tumor can be eradicated in finite time and it does not recur. Hence the decline in TCP after treatment is an artifact of the Poissonian model.

4.3 Dependence of Growth Rate b and Survival Fraction $S(d)$

In order to investigate how the models depend on the tumor growth rate and the radio-sensitivity of the tumor, we compute the TCP for different effective growth rates b and survival fractions $S(d)$. For matters of space we show only protocol C . The behaviour is the same for the other protocols.

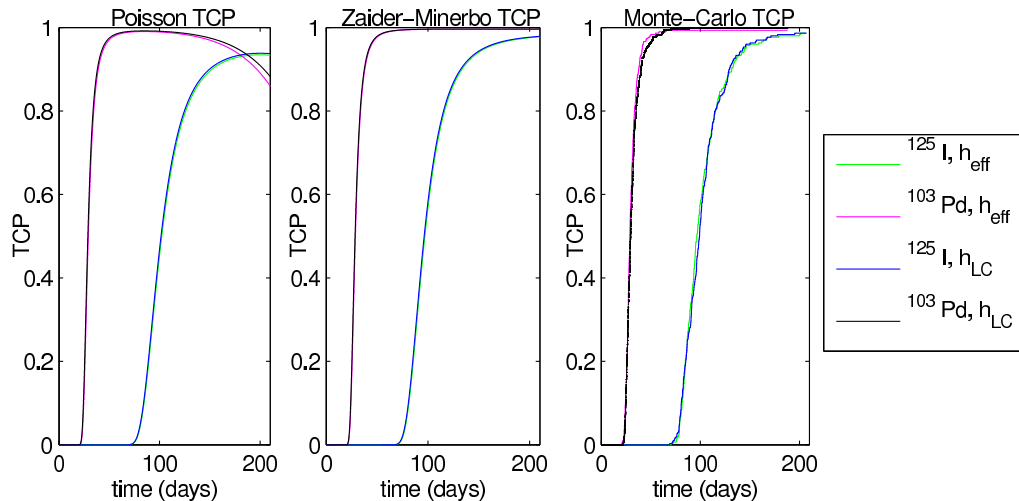


Figure 4.4: TCP as a function of time for permanent seed treatment $^{103}\text{Pd}, ^{125}\text{I}$, with the *effective dose* hazard function (4.37) and the Lea-Catcheside hazard function (4.36). The left panel is for the Poissonian TCP, the middle panel is for the Zaider-Minerbo TCP and the right panel is for the Monte Carlo TCP. Parameter values are from Table 3.2.

We study the TCP dependence on the growth rate in Figure 4.5: In (a) we plot the pairwise distance of the TCP curves between the three one-compartment models as a function of the growth rate in a semilogarithmic plot. We measure the distance in the L^2 -norm, which corresponds to the squared error sum. We see that the distance between Zaider-Minerbo TCP and Poissonian TCP is always smaller than $e^{-2} = 0.14$ when the regrowth rates are in the interval of $[0, 0.07]$, but the distance increases with increasing b , however, it is still very small over all ($< e^{-1}$). The Monte Carlo TCP shows a bigger distance to the other two, but still smaller than e^1 even for the highest growth rate. In Figure 4.5 (b) we record the time when the TCP values reach 95% success. Again the model predictions are very close, with a slight increased difference for large birth rate values.

Now changing the survival fraction by varying the radiosensitivity parameter β , we plot the graphs in Figure 4.6. We show that the $\log-L^2$ distance in Figure 4.6 (a) as a function of survival fraction $S(d)$. Figure 4.6 (b) shows the time at which TCP=95% as a function of $S(d)$. We see from (b) that the time reaching 95% TCP sensitively depends on $S(d)$ but the three models behave the same.

5 Conclusions

We initiated this line of research since we expected, based on experience, that the more complicated models indeed make the same predictions as the simplest model, the Poissonian TCP. Through our systematic study we can confirm this observation. We simulated many more parameter values as presented here and the discrepancy between Poisson models, birth-death models and Monte-Carlo simulations is always small. During our studies we found in the literature that the relation between

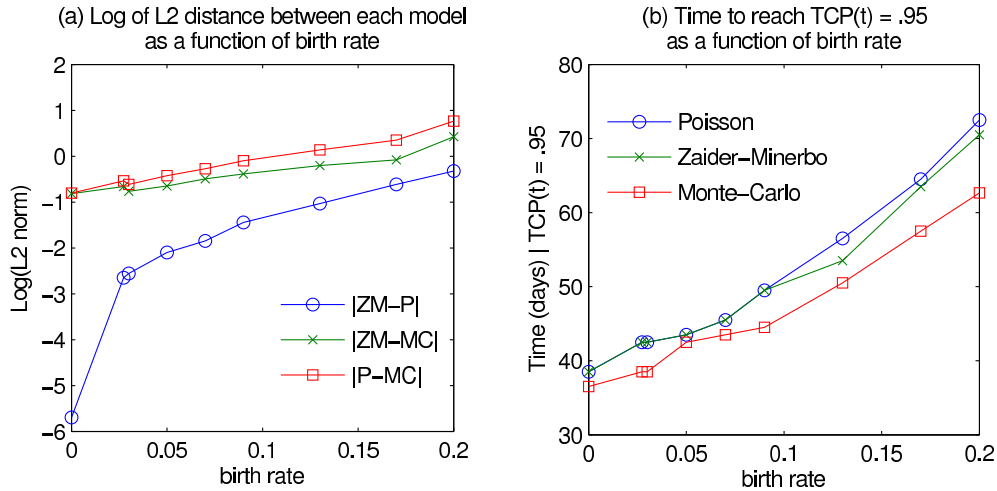


Figure 4.5: (a): Semilogarithmic plot of the pairwise L^2 -distance between the TCP curves as a function of the birth rate b , for treatment protocol C . (b): Time at which the TCP curve reaches 95% as a function of the birth rate b . We use *effective dose* hazard function (2.12)(d) here and all parameters except the birth rate are taken from Table 3.2.

survival fraction and hazard function is often unclear and not well presented. Hence we tried to summarize and compare the different forms of h and $S(D)$ which are discussed in the literature. Different hazard functions are used for fractionated therapies as opposed to brachytherapies. As a side result we found that using the effective interaction window in (2.12)(d), we were able to unify these two approaches into one framework. We showed that (2.12)(d) can equally be applied to fractionated therapies as well as brachytherapies. As for fractionated treatments, it corresponds to the standard fractionated survival fraction and for brachytherapy it corresponds to the Lea-Catchside factor.

The Poisson TCP is simple and computationally efficient. We simulated the three models on the same computer: Intel Core 2 Duo, 2.0GHz, 2GB DDR2. For one typical simulation the Poisson TCP takes 3.34 seconds, the Zaider-Minerbo TCP uses 65.4 seconds and the Monte Carlo TCP uses up to 2.3 hours. Therefore for slow proliferating tumors, we suggest that the Poisson TCP to be used for calculations. However, when birth rate increases, the difference between Poisson TCP and Zaider-Minerbo TCP increases. For example in Figure 4.5 the difference between Poisson and Zaider-Minerbo TCP enlarges to two days when the growth rate is 0.2. This confirms the results of Tucker *et al.* [39], who showed that the Poisson TCP can underestimate the tumor cure up to 15% when the tumor doubling time is 2.06 days (or growth rate 0.34), which is a very fast growing tumor. Furthermore, the change of the survival fraction parameter β will also slightly magnify the difference between the three TCP models.

As for the low dose rate brachytherapy, the Poisson TCP is much more sensitive to the number of the

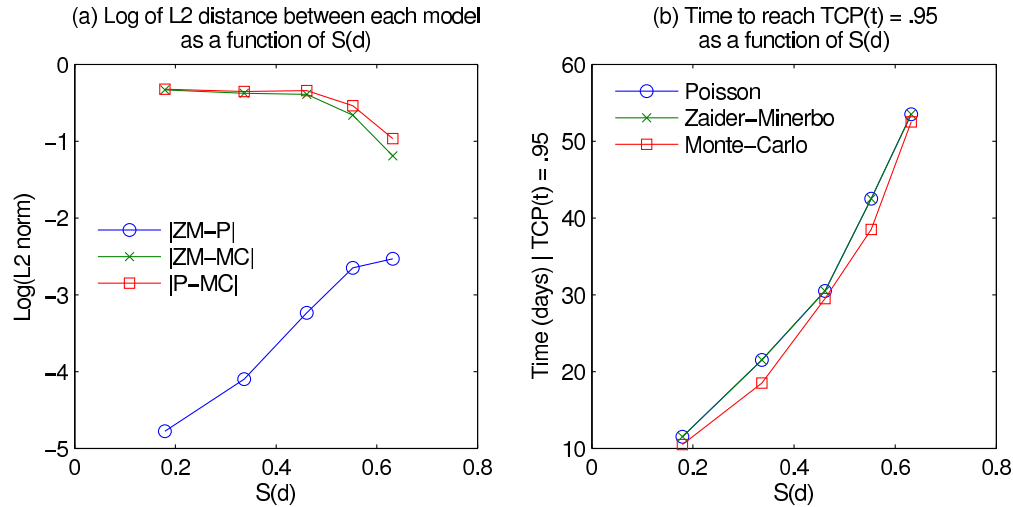


Figure 4.6: (a): Semilogarithmic plot of the pairwise L^2 -distance between the TCP curves for treatment protocol C as function of the survival fraction $S(d)$. (b): Time at which the TCP curve reaches 95% as function of the survival fraction $S(d)$. $S(d)$ is varied by changing β and all other parameters are taken from Table 3.2, *effective dose* hazard function (2.12)(d) is used.

tumor cells. After the end of treatment, the growth of tumor cells (therefore the increase of tumor cell numbers) causes the Poisson TCP to decrease. On the other hand, the Zaider-Minerbo and Monte Carlo TCP remain constant. This is a clear advantage of the stochastic models of Zaider-Minerbo and Monte Carlo. As soon as all cells are eradicated the tumor is gone forever. The Poissonian TCP, however, is based on an ODE formulation. Here solutions only converge to 0 but will never reach 0 in finite time. Hence in the Poissonian formulation a tumor will always recur.

We also compare Poisson, Zaider-Minerbo and Monte Carlo TCP with their corresponding two-compartment TCP models, where the cell cycle effect is included through a quiescent compartment. While the result between the two-compartment models are the same, there is a significant difference between one- and two-compartment models. The two-compartment models give less optimistic predictions and they suggest longer treatment periods. This is related to the fact that quiescent cells are less sensitive to radiation and they can be re-activated by the death of the surrounding active cells. Nutrients become available to the quiescent cells and they enter the cell cycle and re-populate the tumor. Hence it is critical to control the most radio resistant cells.

In this paper we use prostate cancer treatments as test cases for our simulations. We expect, however, that similar conclusions hold true for other localized tumors such as in pancreas, colon, liver, etc.

Overall, the differences in all the models which we study are small. We have to evaluate this within the treatment of a real tumor. There are many important aspects which we do not include in our

models, such as immune response, spatial structure of the tumor, vascularization, metastasis, genetic instabilities, and relevant biochemical pathways. Compared to all these details, which are still missing from the models, the TCP models considered here are basically identical. Our study confirms the usefulness of the Poissonian formulation and we feel that more complicated models should only be used when absolutely necessary.

Abbreviations

TCP - Tumor Control Probability; LQ - Linear Quadratic; ^{125}I - Iodine 125; ^{103}Pd - Palladium 103; LC - Lea-Catcheside; ZM - Zaider-Minerbo; DH - Dawson-Hillen; ODE - ordinary differential equation; TS - Treatment success.

Acknowledgements

We are extremely grateful for a number of highly constructive remarks from Leonid Hanin (Idaho State University), which helped to improve this manuscript. This work is supported by NSERC (Natural Sciences and Engineering Research Council) of Canada and ELAP (Emerging Leaders in the Americas Program).

References

- [1] American cancer society. <http://www.cancer.org/docroot/home/index.asp>.
- [2] Cancer research uk. <http://www.cancerhelp.org.uk/help/default.asp?page=52>.
- [3] B. Basse, B.C. Baguley, E.S. Marshall, W.R. Joseph, B. van Brunt, G. Wake, and D.J.N. Wall. A mathematical model for analysis of the cell cycle in human tumour. *J. Math. Biol.*, 47:295–312, 2002.
- [4] Prostate Cancer Canada. <http://www.prostatecancer.ca/prostate-cancer/prostate-cancer/statistics.aspx>.
- [5] D.J. Carlson, R.D. Stewart, X.A. Li, K. Jennings, J.Z. Wang, and M. Guerrero. Comparison of *in vitro* and *in vivo* α/β ratios for prostate cancer. *Phys. Med. Biol.*, 49:4477–4491, 2004.
- [6] A. Dawson and T. Hillen. Derivation of the tumour control probability (TCP) from a cell cycle model. *Comput. and Math. Meth. in Medicine*, 7:121–142, 2006.
- [7] J.F. Fowler. The linear-quadratic formula and progress in fractionated radiotherapy. *Br. J. Radiol.*, 62:679–694, 1989.

- [8] K. M. Franks, T. M. Bartol, and T. J. Sejnowski. An M-cell model of calcium dynamics and frequency-dependence of calmodulin activation in dendritic spines. *Neurocomputing*, 38:9–16, JUN 2001. 9th Annual Computational Neuroscience Meeting (CNS*00), Brugge, Belgium, Jul, 2000.
- [9] J. Gong, T. Hillen, C. Field, and M. Parliament. Optimal cancer radiotherapy treatment schedules under cumulative radiation effect constraint, 2010. In preparation.
- [10] G. Gonzalez-Parra, A. J. Arenas, and F. J. Santonja. Stochastic modeling with Monte Carlo of obesity population. *Journal of Biological systems*, 18(1):93–108, 2010.
- [11] L. G. Hanin. A stochastic model of tumor response to fractionated radiation: limit theorems and rate of convergence. *Math Biosci*, 91(1):1–17, 2004.
- [12] L. G. Hanin, M. Zaider, and A. Y. Yakovlev. Distribution of the number of clonogens surviving fractionated radiotherapy: a long-standing problem revisited. *Int J Radiat Biol*, 77(2):205–13, 2001.
- [13] L.G. Hanin. Iterated birth and death process as a model of radiation cell survival. *Mathematical biosciences*, 169(1):89–107, 2001.
- [14] T. Hillen, G. de Vries, J. Gong, and C. Finlay. From cell population models to tumour control probability: including cell cycle effects. *Acta Oncologica*, 7:121–142, 2010.
- [15] J. A. Horas, O. R. Olguin, and M. G. Rizzotto. Examining the validity of poissonian models against the birth and death {TCP} models for various radiotherapy fractionation schemes. *Int. J. Radiat. Biol.*, 86:711–717, 2010.
- [16] J. H. A. M. Kaanders, L. A. M. Pop, H. A. M. Marres, I. Bruaset, F. J. A. van den Hoogen, M. A. W. Merks, and A. J. van der Kogel. Arcon: experience in 215 patients with advanced head-and-neck cancer. *Int. J. Radiat. Oncol. Biol. Phys.*, 52:769–778, 2002.
- [17] A.M. Kellerer and H.H. Rossi. The theory of dual radiation action. *Curr. Top. Radiation Res. Q.*, 8:85–158, 1972.
- [18] S. Levegrun, A. Jackson, M. J. Zelefsky, E. S. Venkatraman, M. W. Skwarchuk, W. Schlegel, Z. Fuks, S. A. Leibel, and C. C. Ling. *Risk group dependence of dos-response for biopsy outcome after three-dimensional conformal radiation therapy of prostate cancer*, volume 63. 2002.
- [19] X Allen Li, Jian Z. Wang, Robert D. Stewart, and Steven J. DiBiase. Dose escalation in permanent brachytherapy for prostate cancer: dosimetric and biological considerations. *Physics in Medicine and Biology*, 48:2753–65, 2003.

- [20] Y. Liao, M. Joiner, Y. Huang, and Jay Burmeister. Hypofractionation: What does it mean for prostate cancer treatment? *Brit. J. Radiol.*, 76:260–268, 2010.
- [21] B. Maciejewski, H. R. Withers, J. M. G. Taylor, and A. Hliniak. Dose fractionation and regeneration in radiotherapy for cancer of the oral cavity and oropharynx - tumor dose-response and repopulation. *International Journal of Radiation Oncology Biology Physics*, 16(3):7831–843, 1989.
- [22] K. Mah, J. van Dyk, and P. Y. Poon. Acute radiation induced pulmonary damage: A clinical study on the response to fractionated radiation therapy. *Int. J. Radiat. Oncol. Biol. Phys.*, 13:179–188, 1987.
- [23] A. Maler and F. Lutscher. Cell cycle times and the tumor control probability. *Mathematical Medicine and Biology*, Published On line:1–30, Dec. 2009.
- [24] S. Mathews. Valuing risky projects with real options. *Research-technology Management*, 52(5):32–41, 2009.
- [25] A. McAnaney and S.F.C. O’Rourke. Investigation of various growth mechanisms of solid tumor growth within the linear-quadratic model for radiotherapy. *Phys. Med. Biol.*, 52:1039–1054, 2006.
- [26] S. Nag, D. Beyer, J. Friedland, P. Grimm, and R. Nath. American brachytherapy society (abs) recommendations for transperineal permanent brachytherapy of prostate cancer. *International Journal of Radiation, Oncology, Biology, Physics*, 44(4):789–799, 1999.
- [27] World Health Organization. World cancer report 2008.
- [28] F. O’Rourke, H. McAnaney, and T. Hillen. Linear quadratic and tumour control probability modelling in external beam radiotherapy. *J. Math. Biology*, 58:799–817, 2009.
- [29] J. T. Parsons, W. Mendenhall, N. Cassisi, J. Isascs, and R. R. Million. Accelerated hyperfractionation for head and neck cancer. *International Journal of Radiation, Oncology, Biology, Physics*, 14(5):649–658, 1988.
- [30] S. B. Popov and M. E. Prokhorov. Population synthesis in astrophysics. *Physics-uspekhi*, 50(11):1123–1146, 2007.
- [31] J. M. Prausnitz and F. W. Tavares. Thermodynamics of fluid-phase equilibria for standard chemical engineering operations. *Aiche Journal*, 50(4):739–761, APR 2004.
- [32] A. M. Reuther, T. R. Willoughby, and P.A. Kupelian. Toxicity after hypofractionated external beam radiotherapy (70 gy at 2.5 gy per fraction) versus standard fractionation radiotherapy (78 gy at 2.0 gy per fraction) for localized prostate cancer. *Int. J. Rad. Onc. Biol. Phys.*, 54(Suppl.1):187–188, 2002.

- [33] N. A. Stavreva, P. V. Stavrev, B. Warkentin, and B.G. Fallone. Investigating the effect of cell repopulation on the tumor response to fractionated external radiotherapy. *Med. Phys.*, 30(5):735–742, 2003.
- [34] L. Strigari, M. D’Andrea, A. Abate, and M. Benassi. A heterogeneous dose distribution in simultaneous integrated boost: the role of the clonogenic cell density on the tumor control probability. *Phys. in Med. Biol.*, 53(19):5257–5273, 2008.
- [35] K.R. Swanson, L.D. True, D.W. Lin, K.R. Buhler, R. Vessella, and J.D. Murray. A quantitative model for the dynamics of serum prostate-specific antigens as a marker for cancerous growth. *Am. J. Pathol.*, 158:2195–2199, 2001.
- [36] H. D. Thames, S. M. Bentzen, I. Turesson, M. Overgaard, and W. Vandenbergert. Time-dose factors in radiotherapy - a review of the human data. *Radiotherapy and Oncology*, 19(3):219–235, 1990.
- [37] H. R. Thieme. *Mathematics in Population Biology*. Princeton University Press, 2003.
- [38] E. L. Travis and S. L. Tucker. Isoeffect models and fractionated radiation-therapy. *International Journal of Radiation Oncology Biology Physics*, 13(2):283–287, 1987.
- [39] S. L. Tucker, H. D. Thames, and J. M. G. Taylor. How well is the probability of tumor cure after fractionated-irradiation described by Poisson statistics. *Radiation Research*, 124(3):273–282, 1990.
- [40] J.R. Usher. Mathematical derivation of optimal uniform treatment schedules for the fractionated irradiation of human tumors. *Math. Biosci.*, 49:157–184, 1980.
- [41] T. E. Wheldon. *Mathematical models in cancer research*. Taylor and Francis, 1988.
- [42] H. R. Withers, J. M. G. Taylor, and B. Maciejewski. The hazard of accelerated tumor clonogen repopulation during radiotherapy. *Acta Oncologica*, 27(2):131–146, 1988.
- [43] R. J. Yaes. Linear-quadratic model isoeffect relations for proliferating tumor-cells for treatment with multiple fractions per day. *International Journal of Radiation Oncology Biology Physics*, 17(4):901–905, 1989.
- [44] A. Y. Yakovlev. Comments on the distribution of clonogens in irradiated tumors. *Radiation Research*, 134(1):117–120, 1993.
- [45] Y. Yoshioka, K. Konishi, R. Oh, L. Sumida, H. Yamazaki, S. Nakamura, K. Nishimura, and N. Nonomura. High-dose-rate brachytherapy without external beam irradiation for locally advanced prostate cancer. *Radiotherapy and Oncology*, 80:62–68, 2006.

- [46] M. Zaider and G. N. Minerbo. Tumour control probability: a formulation applicable to any temporal protocol of dose delivery. *Phys. Med. Biol.*, 45:279–293, 2000.